



Discussion

Tuning optical spectrum between Fano and Lorentzian line shapes with phase control

Keyu Xia^{a,*}, Jian-Qi Zhang^b^a ARC Centre for Engineered Quantum Systems, Department of Physics and Astronomy, Macquarie University, NSW 2109, Australia^b State Key Laboratory of Magnetic Resonance and Atomic and Molecular Physics, Wuhan Institute of Physics and Mathematics, Chinese Academy of Sciences, and Wuhan National Laboratory for Optoelectronics, Wuhan 430071, China

ARTICLE INFO

Article history:

Received 9 April 2015

Received in revised form

6 May 2015

Accepted 20 May 2015

Available online 26 May 2015

Keywords:

March–Zehnder interferometer

Phase control

Lorentzian profile

Fano profile

ABSTRACT

Controlling the spectrum of light with a phase has received intensive interest of researchers recently. Here, we study the phase control of the spectral line shape of the output from an optical March–Zehnder interferometer (MZI) with one arm involving a high quality Fabry–Perot cavity. Due to the interaction of the narrow-band light transmitted through the cavity with the broadband light, the spectrum can be tuned from Lorentzian to Fano-like profile with a phase shifter in MZI.

© 2015 Elsevier B.V. All rights reserved.

1. Introduction

Fano resonance corresponding to Fano absorption line shapes is a result of the quantum interference originated from the coupling of a discrete energy state (discrete light mode) to continuum of states (lights with continuous spectrum) [1,2]. Typical asymmetric Fano absorption line shapes have been widely studied throughout atomic ionization [3], classical harmonic oscillators [4], light propagation in photonic devices [5,6] and optomechanical system recently [7]. Since Lorentzian profile is the natural line shape due to the quantum system decay, the transition from symmetric Lorentzian (Fano parameter $|q| \rightarrow \infty$) to asymmetric Fano profile (finite Fano parameter q) is of interest in fundamental physics and also promises important applications [8,9]. Fano spectrum can be engineered by tuning the coupling strength between a discrete state and a continua [10,11]. More interestingly, tuning spectrum between Lorentzian and Fano line shapes via a phase shift [3,12,13] reveals deep physics in quantum mechanics, which attracts much interests recently.

In this paper, we present a simple, all-optical MZI configuration for demonstrating the phase control of the spectra between Lorentzian and Fano profiles. The narrow-band transmission (discrete mode) of a high-quality Fabry–Perot (FP) cavity interferes with the

broadband laser beam on the second beam splitter of March–Zehnder interferometer (MZI). This quantum interference results in a spectral line shape dependent on the relative phase shift between the light beams.

2. Setup and model

The system under our consideration is plotted in Fig. 1, where a coherent laser beam incidents into a highly reflective beam splitter (BS1) [14] and is split into two beams with one beam passing through a high-Q optical cavity and the other experiencing a phase shift θ . Then the two output beams are mixed at the second BS2, and we monitor one of the outputs from the BS2.

Let us consider the line shape of the beam \hat{a}_4 detected by the detector D1. We assume the input laser beam \hat{a}_0 with frequency ω_{in} and the BS1 with the reflection $\eta^2 \approx 0$. The other input \hat{a}_1 is a vacuum field, and hence its normally ordered correlation is zero, i.e. $\langle \hat{a}_1^\dagger(-\Omega)\hat{a}_1(\omega) \rangle = 2\pi\bar{n}_{th}\delta(\Omega + \omega)$ with the thermal excitation $\bar{n}_{th} \approx 0$. Thus the upper and lower beams output from the BS1 are, respectively, given by

$$\hat{a}_2 = i\sqrt{1-\eta^2}\hat{a}_1 + \eta\hat{a}_0, \quad (1a)$$

$$\hat{a}_3 = \eta\hat{a}_1 + i\sqrt{1-\eta^2}\hat{a}_0. \quad (1b)$$

* Corresponding author.

E-mail address: xiakeyu@gmail.com (K. Xia).

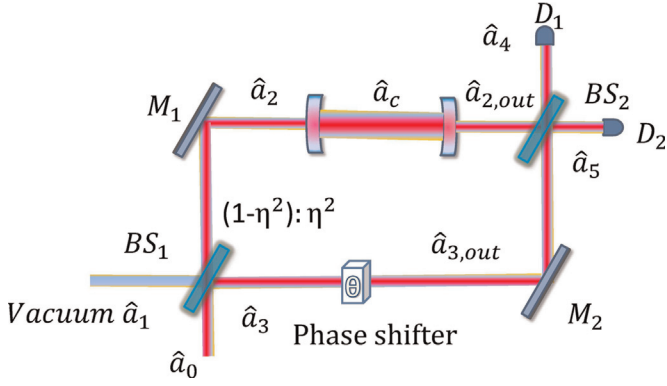


Fig. 1. Setup for tuning the output spectral profile with phase shift. A laser beam \hat{a}_0 is split by the first BS into the upper and lower beams. Another input \hat{a}_1 of this BS is vacuum field. The phase of the lower one is shifted by θ , while the upper one passes through an optical cavity with a negligible intrinsic loss $\kappa_i \approx 0$. Then the two beams are mixed via the second BS to beams \hat{a}_4 and \hat{a}_5 , and then detected by detectors 1 and 2. The first beam splitter is highly reflective such that the reflection $\eta^2 \approx 0$.

The upper beam \hat{a}_2 drives an optical cavity mode \hat{a}_c with a coupling strength κ_{ex} and the cavity mode leaks out to the MZI with two identical rates κ_{ex} from two sides. For the cavity with a resonance frequency ω_c and a total decay rate $\kappa = 2\kappa_{ex}$, the dynamics of the cavity field is governed by

$$\hat{a}_c = (-i\omega_c - \kappa)\hat{a}_c + 2\kappa_{ex}\hat{a}_2. \quad (2)$$

According to the input–output relation, we have the output field in the steady state [15]

$$\hat{a}_{2,out}(\omega) = \frac{-2\kappa_{ex}\sqrt{1-\eta^2}\hat{a}_1(\omega) + 2i\kappa_{ex}\eta\hat{a}_0(\omega)}{(\omega - \omega_c) + i\kappa}. \quad (3)$$

On the other hand, the lower beam going through the tunable phase shifter becomes

$$\hat{a}_{3,out}(\omega) = e^{i\theta}(\eta\hat{a}_1(\omega) + i\sqrt{1-\eta^2}\hat{a}_0(\omega)). \quad (4)$$

The two beams are mixed at a 50:50 beam splitter (BS2), yielding the output

$$\begin{aligned} \sqrt{2}\hat{a}_4(\omega) &= \hat{a}_{3,out}(\omega) + i\hat{a}_{2,out}(\omega) = \left(\eta e^{i\theta} - \frac{2i\kappa_{ex}\sqrt{1-\eta^2}}{(\omega - \omega_c) + i\kappa} \right) \hat{a}_1(\omega) \\ &+ \left(i\sqrt{1-\eta^2}e^{i\theta} - \frac{2\eta\kappa_{ex}}{(\omega - \omega_c) + i\kappa} \right) \hat{a}_0(\omega), \end{aligned} \quad (5)$$

whose spectrum is defined as $\langle \hat{a}_4(-\Omega)\hat{a}_4(\omega) \rangle = 2\pi S_4(\omega)\delta(\omega + \Omega)$. Note that the vacuum field \hat{a}_1 only adds small noise of a level of vacuum fluctuation to the output spectrum $S_4(\omega)$. For our optical

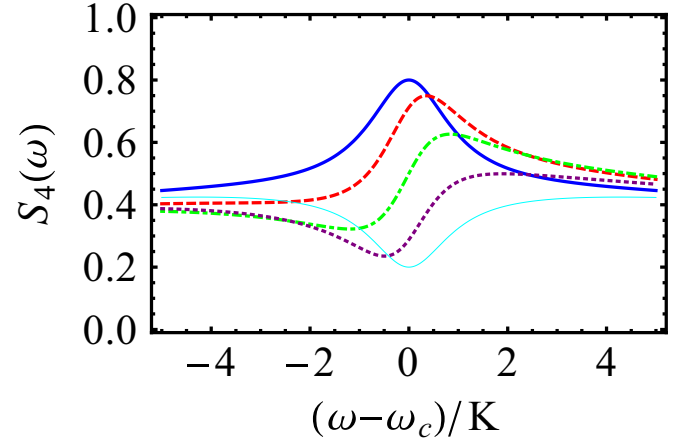


Fig. 3. Output of the power spectra for different phase shift $\theta = \{0, \pi/4, \pi/2, 3\pi/4, \pi\}$ corresponding to $q \approx \{4/3e^{0.5\pi i}, 1.26e^{0.44\pi i}, 1.05e^{0.40\pi i}, 0.8e^{0.40\pi i}, 2/3e^{0.5\pi i}\}$, shown by (solid blue line, dashed red line, dotted-dashed green line, dotted purple line and thin cyan line). $\eta_n = 25\kappa$. (For interpretation of the references to color in this figure caption, the reader is referred to the web version of this paper.)

MZI, we consider the case of a strong input, $\eta^2\langle \hat{a}_0^\dagger(\omega)\hat{a}_0(\omega) \rangle \gg 2\pi(1-\eta^2)\bar{n}_{th}$ that

$$\hat{a}_4(\omega) \approx \frac{1}{\sqrt{2}} \left(i\sqrt{1-\eta^2}e^{i\theta} - \frac{2\eta\kappa_{ex}}{(\omega - \omega_c) + i\kappa} \right) \hat{a}_0(\omega). \quad (6)$$

Therefore, to a good approximation, the detected spectrum $S_4(\omega)$ only depends on the coherent input spectrum $\langle \hat{a}_0(-\Omega)\hat{a}_0(\omega) \rangle = 2\pi S_n(\omega)\delta(\omega + \Omega)$. We obtain $S_4(\omega) = \frac{1}{2}\mathcal{T}(\omega - \omega_c)S_n(\omega)$ with the transmission $\mathcal{T} = |i\sqrt{1-\eta^2}e^{i\theta} - 2\eta\kappa_{ex}/((\omega - \omega_c) + i\kappa)|^2$ yielding a standard Fano resonance [1,3]

$$\mathcal{T} = \sigma_0 \frac{|q + \epsilon|^2}{1 + \epsilon^2}, \quad (7)$$

with $\sigma_0 = (1-\eta^2)$, $\epsilon = (\omega - \omega_c)/\kappa$ and $q(\theta) = i + i(2\kappa_{ex}/\kappa)(\eta\sqrt{1-\eta^2})e^{-i\theta}$. Throughout our investigations below, we are interested in the critical coupling such that $\kappa = 2\kappa_{ex}$, and subsequently $q(\theta) \approx \eta \sin \theta + i(1 + \eta \cos \theta)$. Clearly, Fano parameter q representing the line shape is crucially dependent on the phase shift θ . Further decomposing Eq. (6), we have

$$\mathcal{T} = T_0 + T_1 + T_{Lorentz} + T_{Fano}, \quad (8)$$

where

$$T_0 = (1 - \eta^2) \quad (9a)$$

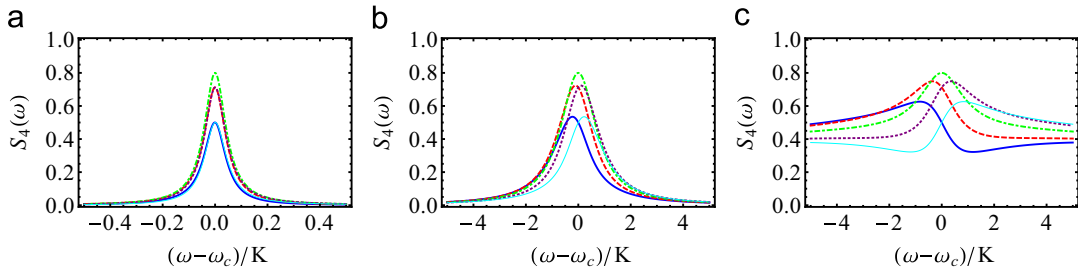


Fig. 2. Phase control of the scaled power spectral profiles for different linewidths of the input laser beam (a) $\eta_n = 0.05\kappa$, (b) $\eta_n = \kappa$, (c) $\eta_n = 25\kappa$. Spectra with different phase shifts are shown by {solid blue lines, red dashed lines, dotted-dashed green lines, dotted purple lines and thin solid lines} for $\theta = \{-\pi/2, -\pi/4, 0, \pi/4, \pi/2\}$ corresponding to $q \approx \{1.054e^{0.6\pi i}, 1.258e^{0.56\pi i}, 4/3e^{0.5\pi i}, 1.26e^{0.44\pi i}, 1.054e^{0.40\pi i}\}$. (For interpretation of the references to color in this figure caption, the reader is referred to the web version of this paper.)

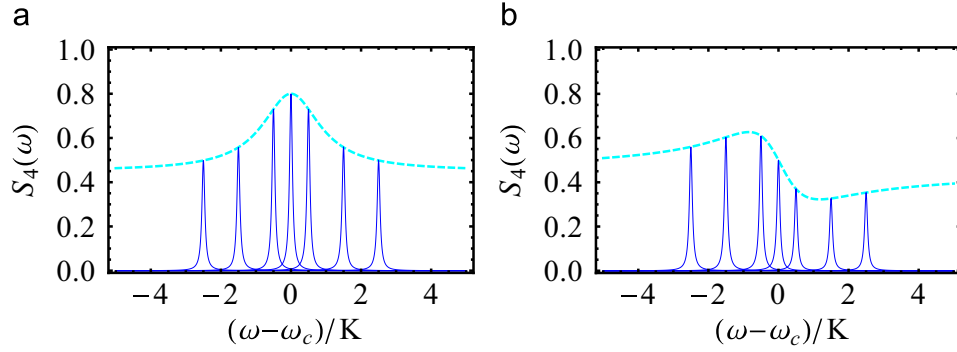


Fig. 4. Output of the power spectra for different input laser frequencies with a narrow linewidth $\gamma_{in} = 0.05\kappa_{ex}$. (a) $\theta=0$, (b) $\theta = -\pi/2$. The thick dashed lines are the envelope of the amplitude of the output spectra for different input frequencies ω_{in} . From left to right, δ increases from -2.5κ to 2.5κ .

$$T_1 = \left(\frac{2\kappa_{ex}}{\kappa} \right)^2 \frac{\eta^2}{1 + \epsilon^2} \quad (9b)$$

$$T_{\text{Lorentz}} = \frac{2\kappa_{ex}}{\kappa} \frac{2\eta\sqrt{1-\eta^2}\cos\theta}{1 + \epsilon^2} \quad (9c)$$

$$T_{\text{Fano}} = \frac{2\kappa_{ex}}{\kappa} \frac{2\eta\sqrt{1-\eta^2}\sin\theta}{1 + \epsilon^2}, \quad (9d)$$

where the first term T_0 is trivial and the second term T_1 is negligible for $\eta^2 \approx 0$. Only the latter two terms, involving the phase shift θ , are of interest. T_{Lorentz} indicates a Lorentzian line shape, and T_{Fano} crucially contributes to Fano profile. The weight of these two contributions can be tuned from 0 to 1 by changing the phase shift θ from 0 to $\pi/2$. The input laser spectrum modulated by this phase-controllable transmission yields the output line shape. From now on, we assume that the input laser beam is initially of Lorentzian profile, i.e., $S_{in}(\omega) = \gamma_{in}^2 / ((\omega - \omega_{in})^2 + \gamma_{in}^2)$ with a linewidth of γ_{in} , and the detuning between the cavity and the input laser is given by $\delta = \omega_c - \omega_{in}$. We show below the possibility to control the output spectral profile by tuning the phase shift θ based on Eqs. (8) and (9).

3. Results

Now we go to investigate how the phase shift θ modify the output power spectrum between the Lorentzian and Fano profiles.

Fig. 2 plots some output spectral profile of port 4 for on-resonance excitation $\delta=0$. In Fig. 2(a), the input laser spectrum is much narrower than the linewidth (κ) of the cavity, i.e., $\gamma_{in} = 0.05\kappa$. In this case, the detuning ϵ is negligibly small over the input laser spectrum. The transmission coefficient \mathcal{T} only modulates the amplitude of the output spectrum. As a result, the spectrum line shape is mainly determined by the input laser spectrum and remains Lorentzian with its amplitude modulated by $\cos(\theta)$. It can be clearly seen from Fig. 2(a) that the spectrum for $\theta=0$ has the maximum amplitude, while the spectra for $\theta = -\pi/2, -\pi/4$ overlap with those for $\theta = \pi/2, \pi/4$, respectively. When the input laser spectrum increases to be comparable to the linewidth of the cavity, e.g. $\gamma_{in} = \kappa$ as shown in Fig. 2(b), the output spectrum starts to deform from Lorentzian shape. Except the change in the amplitude of spectra as the phase shift θ increasing, the peaks also shift.

Further considering the input laser with the band much broader than that of the cavity, we find that the output spectrum can transit from Lorentzian to Fano profile controlled by the phase shift θ , see Fig. 2(c). In the case of $\gamma_{in} = 25\kappa$, the spectral line shape varies from the Fano to the Lorentzian with $\theta = -\pi/2 \rightarrow 0$, and

then turns back to the Fano when θ is tuned to $\pi/2$. Interestingly, besides the profile change, the peak of the output spectrum shifts accordingly when the phase θ changes. For example, when $\theta=0$ corresponding to $q = 4/3i$, the spectrum is a Lorentzian profile located at $\omega = \omega_c$ but offset by ~ 0.45 . For $\theta = -\pi/2$ corresponding to $q = 1.054e^{0.6\pi i}$ ($1.054e^{0.4\pi i}$), the spectral peak shifts left (right) by $\sim 2\kappa/3$. At the same time, the spectral profile becomes Fano. This amount of spectral shift is large enough to be detected.

So far, we have studied the output spectral profile as the Fano contribution T_{Fano} varies from maximal negative value to maximal positive. We now investigate how the spectral profile changes when the Lorentzian contribution changes from maximal negative value to maximal positive. As shown in Fig. 3, the phase θ is tuned from 0 to π . As a result, the spectral profile is modified from a normal Lorentzian profile, $\theta=0$, to Fano, $\theta = \pi/2$, and then to a reversed Lorentzian, $\theta=\pi$.

Note that the output power spectra are Lorentzian or Fano profile overlapping on the broadband power spectrum of the input laser. This phase tunable spectrum attributes to the quantum interference between a narrow band field and a broadband field. Such phase dependent transition of the spectral profile has been demonstrated in ionization of atoms by a ultrastrong laser [3] and in deformed optical cavity [12,16] as well. In contrast, we can tune the profile between the Fano and the Lorentzian by means of phase shift even though the absolute of Fano parameter q is small. More interestingly, the change in the relative phase θ can shift the peaks of the output spectra. If the phase shifter is inserted between two highly reflective mirrors as in [17], which cause a N -fold enhanced total phase shift $N\theta$ with $N \gg 1$, our scheme provides a novel way to measure the small phase shift by monitoring the position of spectral peaks (Fig. 4).

For a more general case, i.e., $\delta \neq 0$, the situation is more complicated, but more interesting. For example, starting from $\gamma_{in} \ll \kappa$ with $\theta=0$, the output spectrum is always a Lorentzian profile. But, by scanning the input laser in the vicinity of the cavity resonance frequency, the spectrum amplitude follows an envelope, which is phase tunable. As shown in Fig. 4, the modulation of the spectral amplitude at different detuning δ can be switched between Lorentzian and Fano profiles.

4. Conclusion

In summary, we have demonstrated an all-optical version of phase control of the spectral line shape between Fano and Lorentzian profiles. Our system involves a simple MZI in which one of the arms includes an optical cavity. To observe the phase tunable spectral line shapes, the first BS1 need to be highly reflective and the spectrum of the input laser is required to span a band much broader than the linewidth of the cavity. Moreover, we found that

the position output spectrum is dependent on the phase shift. Thus, our findings opens a way to detect a small phase shift by monitoring the position of the output spectrum.

Acknowledgement

K.X. would like to thank the support from the Australian Research Council Centre of Excellence for Engineered Quantum Systems (EQUS), project number, CE110001013. J.Q.Z. thanks for the discussion with Prof. Mang Feng, Dr. Wei Wan and Dr. De-Zhi Xiong. This work was also supported by the China Postdoctoral Science Foundation (Grant nos. 2013M531771 and 2014T70760) and the National Natural Science Foundation of China (Grant nos. 11204080, 11304366 and 91421111).

References

- [1] U. Fano, *Phys. Rev.* 124 (1961) 1866.
- [2] A.E. Miroshnichenko, S. Flach, Y.S. Kivshar, *Rev. Mod. Phys.* 82 (2010) 2257.
- [3] C. Ott, A. Kaldun, P. Raith, K. Meyer, M. Laux, J. Evers, C.H. Keitel, C.H. Greene, T. Pfeifer, *Science* 340 (2013) 716.
- [4] Y.S. Joe, A.M. Satanin, C.S. Kim, *Phys. Scr.* 74 (2006) 259.
- [5] A.E. Miroshnichenko, Y. Kivshar, C. Etrich, T. Pertsch, R. Iliew, F. Lederer, *Phys. Rev. A* 79 (2009) 013809.
- [6] N. Verellen, Y. Sonnefraud, H. Sobhani, F. Hao, V.V. Moshchalkov, P.V. Dorpe, P. Nordlander, S.A. Maie, *Nano Lett.* 9 (2009) 1663.
- [7] K. Qu, G.S. Agarwal, *Phys. Rev. A* 87 (2013) 063813.
- [8] S. Chen, S. Jin, R. Gordon, *Phys. Rev. X* 4 (2014) 031021.
- [9] S.M. Cavaletto, Z. Harman, C. Ott, C. Buth, T. Pfeifer, C.H. Keitel, *Nat. Photon.* 8 (2014) 520.
- [10] M. Galli, S.L. Portalupi, M. Belotti, L.C. Andreani, L. O'Faolain, T.F. Krauss, *Appl. Phys. Lett.* 94 (2009) 071101.
- [11] Y. Yu, M. Heuck, H. Hu, W. Xue, C. Peucheret, Y. Chen, L.K. Oxenløwe, K. Yvind, J. Mørk, *arxiv:1404.7532*.
- [12] Y.-F. Xiao, X.-F. Jiang, Q.-F. Yang, L. Wang, K. Shi, Y. Li, Q. Gong, *Laser Photon. Rev.* 7 (2013) L51.
- [13] N. Huang, L.J. Martínez, M.L. Povinelli, *Opt. Express* 21 (2013) 20675.
- [14] A.I. Lvovsky, S.A. Babichev, *Phys. Rev. A* 66 (2002) 011801(R).
- [15] G.S. Agarwal, S. Huang, *Phys. Rev. A* 85 (2012) 021801(R).
- [16] Q.-F. Yang, X.-F. Jiang, Y.-L. Cui, L. Shao, Y.-F. Xiao, *Phys. Rev. A* 88 (2013) 023810.
- [17] B.L. Higgins, D.W. Berry, S.D. Bartlett, H.M. Wiseman, G.J. Pryde, *Nature* 450 (2007) 393.